

Substrate Engineering Enabling Fluorescence Droplet Entrapment for IVC-FACS-Based Ultrahigh-Throughput Screening

Fuqiang Ma,[†] Michael Fischer,^{‡,§} Yunbin Han,[†] Stephen G. Withers,[‡] Yan Feng,[†] and Guang-Yu Yang^{*,†,‡,#}

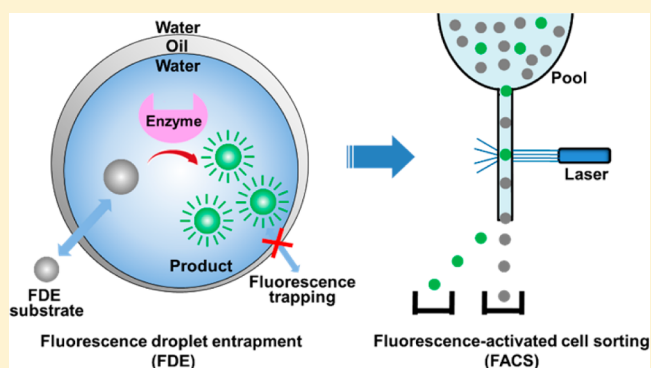
[†]State Key Laboratory of Microbial Metabolism, School of Life Sciences and Biotechnology, Shanghai Jiao Tong University, 800 Dongchuan Road, Shanghai 200240, China

[‡]Department of Chemistry, University of British Columbia, 2036 Main Mall, Vancouver, British Columbia V6T 1Z1, Canada

[#]Shanghai Collaborative Innovation Center for Biomanufacturing (SCICB), East China University of Science and Technology, 130 Meilong Road, Shanghai 200237, China

S Supporting Information

ABSTRACT: In vitro compartmentalization-based fluorescence-activated cell sorting (IVC-FACS) is a powerful screening tool for directed evolution of enzymes. However, the efficiency of IVC-FACS is limited by the tendency of the fluorescent reporter to diffuse out of the droplets, which decouples the genotype and phenotype of the target gene. Herein we present a new strategy called fluorescence droplet entrapment (FDE) to solve this problem. The substrate is designed with a polarity that enables it to pass through the oil phase, react with the enzyme and generate an oil-impermeable and fluorescent product that remains entrapped inside the droplet. Several FDE substrates were designed, using two distinct substrate engineering strategies, for the detection of phosphotriesterases, carboxylesterases, and glycosidases activities. Model screening assays in which rare phosphotriesterase-active cells were enriched from large excesses of inactive cells showed that the enrichment efficiency achievable using an FDE substrate was as high as 900-fold: the highest yet reported in such an IVC-FACS system. Thus, FDE provides a means to tightly control the onset of the enzymatic reaction, minimize droplet cross-talk, and lower the background fluorescence. It therefore may serve as a useful strategy for the IVC-FACS screening of enzymes, antibodies, and other proteins.



Directed evolution is a powerful approach for tailoring enzymes and other proteins with enhanced activity, desired specificity, and high stability.^{1,2} However, the success of a directed evolution experiment largely relies on the efficiency of the screening method employed. Recently, in vitro compartmentalization-based fluorescence-activated cell sorting (IVC-FACS) has become one of the most powerful techniques for high-throughput screening of enzymes.^{3,4} IVC-FACS encapsulates the enzyme-encoding gene, the enzyme, and its fluorescent product in the same monodisperse picoliter water-in-oil-in-water (w/o/w) droplet, thereby creating a microreactor that couples the genotype and phenotype of the target gene. The biological activity inside these microreactors can be measured and sorted using a benchtop flow cytometer in an ultrahigh-throughput manner ($>10^7$ events/h), allowing the exploration of a vast protein sequence space in a short period of time. In the past several years, IVC-FACS has shown remarkable promise for screening of various kinds of enzymes, including thiolactonase,³ β -galactosidase,⁴ cellulase,⁵ β -glucosidase,⁶ glucose oxidase,⁷ cutinase,⁸ protease,⁹ G-type nerve agent hydrolase,¹⁰ and esterase activities.¹¹

It is crucial for an IVC-FACS system to retain the fluorescent signals inside these microreactors such that information on the

reaction progress can be retrieved over several hours of screening. However, there are two processes that degrade the chemical integrity of the droplets. Small chemicals can rapidly (i) diffuse out of the droplet by partitioning into the carrier oil^{12,13} or (ii) exchange between adjacent droplets through micellar transport.^{14,15} The cross-talk between droplets results in variable concentrations of reaction components inside droplets and breaks the linkage between genotype and phenotype, which decreases the screening accuracy. The cross-talk can be reduced by inclusion of additives such as BSA in the inner aqueous phase¹⁶ or by using fluorinated oils.^{17,18} However, signal loss as a result of diffusion/exchange is still too rapid for some widely used fluorophores, such as 7-hydroxy-4-methylcoumarin and 3-cyano-7-hydroxy-4-methylcoumarin.^{10,19} Sulfonates have been used to increase the water-solubility of the fluorophore, which significantly improves the signal stability in the droplet-based assays.^{20,21} However, the charged sulfonate group now present within the substrate molecule creates problems in its delivery into the droplet as it

Received: May 1, 2016

Accepted: August 5, 2016

Published: August 5, 2016

can no longer diffuse through the oil phase. Since most current IVC-FACS systems use homogenizing or membrane-extrusion techniques to generate the w/o/w microreactors, the substrates would have to be mixed with the cells **before** droplet formation. Consequently, this would result in a high fluorescence background and lower the resolution of the screening, especially for enzymes with high reaction rates.

A strategy that delivers substrate across the oil layer into the inner water phase could solve this problem. Ostafe et al. reported the delivery of a hydrophilic substrate through the oil phase by introducing a hydrophobic group onto the substrate molecule.⁷ Combining the idea of hydrophobic droplet delivery and charged droplet retention, we developed a new strategy by designing a substrate that itself is hydrophobic but that can release a charged fluorophore upon enzymatic cleavage. We name this strategy fluorescence droplet entrapment (FDE).

FDE substrates are designed to be hydrophobic enough to pass through the oil phase into the inner water phase of the microreactor where they are converted by the target enzyme, generating a fluorescent product that is impermeable to the oil phase. Such a substrate could thus be added to the outer water phase **after** the encapsulation of single cells. This approach would eliminate the contact of substrate and enzyme before droplet formation, thereby tightly controlling the onset of the reaction, minimizing droplet cross-talk, lowering the background fluorescence, and improving the accuracy of the IVC-FACS system.

In this work, we describe two substrate engineering strategies for the design of FDE substrates using three different enzyme systems that have each been the focus of considerable work in this field, phosphotriesterases, glycosidases, and esterases. As a first step, we determined the influence of hydrophobicity on the oil-phase permeability of different coumarin derivatives and their corresponding phosphotriesterase substrates. This allowed the selection of one derivative with desired properties, which was then shown to exhibit a clear FDE effect. To improve upon the FDE effect of the first engineering strategy, we further developed a second class of FDE substrates that are themselves neutral and exhibit very low fluorescence but can release a charged fluorophore upon cleavage by the target enzymes. Two glycosides and one ester containing this fluorophore were synthesized as substrates, and their FDE performance in IVC-FACS system was assessed using two glycosidases and an esterase, respectively.

■ EXPERIMENTAL SECTION

Synthesis. The syntheses of fluorogenic phosphotriester substrates derived from 3-cyano-7-hydroxy-4-methylcoumarin (CHMC, **4**), 7-hydroxycoumarin-3-carboxylic acid (HCCA, **6**), and 7-hydroxycoumarin-4-methanesulfonic acid (HCMS, **13**) are described in [Supporting Information S1](#). The syntheses of the fluorogenic ester substrate (**14**) and the fluorogenic galactosyl and glucosyl substrates (**15a** and **15b**) are described in [Supporting Information S2](#).

The log *D* (partition coefficient) values were predicted by using the online ACD/I-Lab prediction engine (ACD/I-Lab 2.0, v5.0.0.184, <https://ilab.acdlabs.com/iLab2/index.php>).

Cleavage of 1, 2, and 3 by Phosphotriesterase GkaP and Mutants. The wild-type phosphotriesterase from *Geobacillus kaustophilus* HTA426 (GkaP) and three of its higher activity mutants 26A8, 26A8Y, and 26A8C were expressed and purified as described previously.²² Enzymatic activity for paraoxon-ethyl (Sigma) was measured spectrophotometrically

at 405 nm by the release of 4-nitrophenol using a UV-2550 spectrometer (Shimadzu). Enzymatic activities for substrate **1**, **2**, and **3** ([Figure 1](#)) were measured using an F-7000 Fluorescence Spectrophotometer (Hitachi) with Ex/Em values at 385/450 nm, 400/450 nm, and 340/467 nm, respectively. One unit (U) of enzyme was defined as the amount of protein that catalyzed the conversion of 1 micro mole of substrate per minute. All the reactions were carried out in 1× PBS (pH 7.4) and were monitored in continuous fashion using a final substrate concentration of 0.2 mM. The enzymatic activity was calculated through the slope of the reaction time course using the corresponding absorption or fluorescence emission coefficients. The molar absorption coefficient of 4-nitrophenol was 16000 L/(mol·cm), and the fluorescence emission coefficients of **4**, **6**, and **13** (the reaction products of substrate **1**, **2**, and **3**, respectively) were measured as 2554 RFU/μM, 3992 RFU/μM, and 504 RFU/μM, respectively (see [Supporting Information S3 and S4](#) for details).

To test the permeability of the substrates through the *E. coli* membrane, the catalytic activities of intact GkaP-26A8 expressing cells and cell lysates were measured. The cell lysate was prepared by mixing 50 μL of cell suspension (in PBS, OD₆₀₀ = 5.0) with 50 μL Bugbuster (Merck) and incubating at 37 °C for 10 min. The enzymatic activity was determined using 100 μL of cell lysate or equivalent cell suspension in a 1.5 mL Eppendorf tube containing 400 μL of PBS; the substrate was then added to a final concentration of 0.2 mM. After incubation at 37 °C for 2 h, the fluorescence of the reaction product was visualized under UV light ([Supporting Information S5](#)).

Retention of Modified Coumarin Fluorophores in Droplets. Compounds **4**, **6**, and **13** were dissolved in 1× PBS (pH 7.4) at a concentration of 100 μM and encapsulated into w/o/w double emulsion droplets using the membrane-extrusion method described previously.¹¹ To mimic the conditions of flow cytometry sorting, the emulsions were diluted 100-fold in the outer water phase and incubated at room temperature. The retention behavior of each compound was investigated by monitoring the fluorescence intensities of the droplets at different incubation times. For fluorescence detection, diluted emulsions were loaded into a flow cytometer (BD FACSAria II) operated by the BD FACSDiva software. The detection threshold was set at FSC > 10 000 and SSC > 10 000. The fluorescence of **4**, **6**, and **13** was detected in the DAPI channel (excitation at 375 nm and the band-pass filter of PMT set at 450/40 nm).

Single-Cell Enzymatic Reaction in w/o/w Double Emulsion Droplets. *E. coli* cells expressing GkaP and its mutants were encapsulated into w/o/w double emulsion droplets using the membrane-extrusion method described previously.¹¹ To initiate the enzymatic reaction, substrates **1** and **2** were added to the outer water phase at final concentrations of 0.5 mM. Since substrate **3** required cell lysis in order to commence the enzymatic reaction (impermeable to *E. coli* cell membrane, [Supporting Information S5](#)), additional experiments involving cell lysis were performed. Before droplet generation, substrate **3** was mixed with the cell suspension at a final concentration of 0.5 mM. The w/o/w double emulsion was then mixed with an equal volume of cell lysate reagent BugBuster (Merck) for cell lysis and incubated at 37 °C, shaken at 500 rpm for 30 min, and then stored on ice. For flow cytometry assays, the reaction systems were diluted 100-fold in the outer water phase and the fluorescence of **4**, **6**, and **13** was measured as described above.

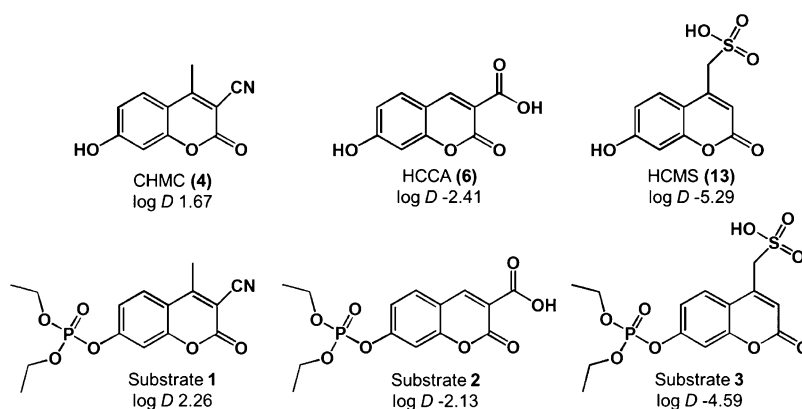


Figure 1. Coumarin derivatives and their corresponding phosphotriester substrates. The molecular hydrophobicities (log D values) at pH 7.4 were predicted using the online ACD/I-Lab prediction engine.

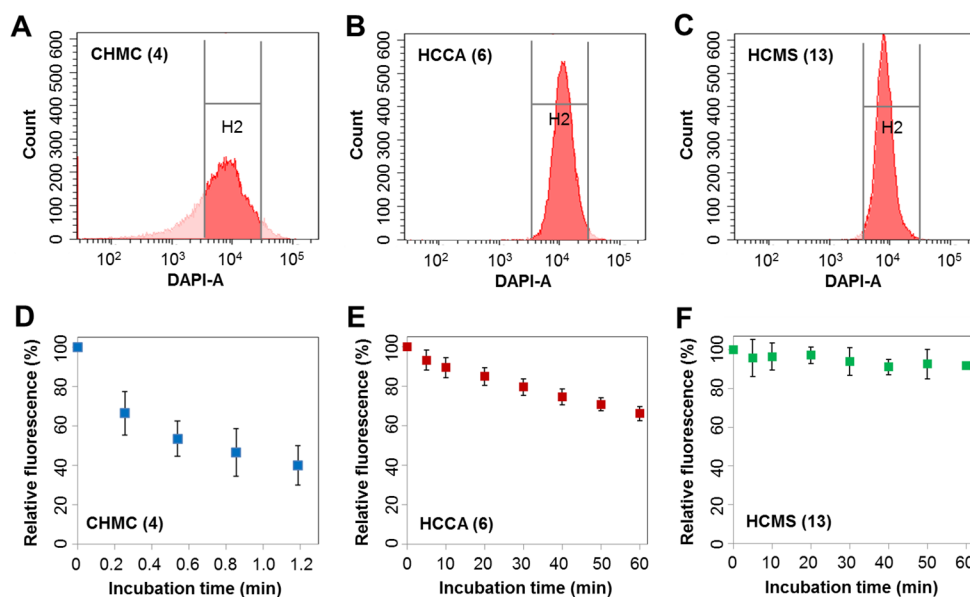


Figure 2. Retention of coumarin derivatives with different hydrophilities in the w/o/w double emulsion droplets. All the fluorophores were encapsulated in the inner water phase at a final concentration of 100 μ M. Before loading on the flow cytometer, the droplets were diluted 100-fold in the outer water phase and incubated at room temperature for different periods of time. (A–C) Fluorescence histograms of droplets encapsulating 4, 6, and 13 at 0 min of incubation. Populations with a fluorescence variation less than 3-fold compared to the mean fluorescence intensity are highlighted (H2 populations); (D–F) Time-dependent fluorescence changes of 4, 6, and 13, respectively. Approximately 20 000 droplets were analyzed for each sample.

Enrichment Analysis of GkaP-26A8-Expressing Cells.

To control the cell number in the droplets, a mCherry fluorescent protein and GkaP coexpression system was constructed (Supporting Information S6). To generate the GkaP-26A8-mCherry-pUC18 plasmid, the genes encoding for the red fluorescence protein mCherry and GkaP-26A8 were inserted along with their individual *rbs* sequences, into the pUC18 vector under control of the same promoter. When the GkaP-26A8-mCherry-pUC18 plasmid was transformed into *E. coli* 10G, both genes were expressed simultaneously, allowing the number of cell-containing droplets to be monitored through their mCherry fluorescence signals.

Cells expressing GkaP-26A8 (*E. coli* 10G strain coexpressing GkaP-26A8 and mCherry fluorescence protein) and GkaP-inactive cells (*E. coli* 10G strain harboring only mCherry-pUC18 plasmid) were mixed at ratios of 1:10, 1:100, and 1:1000 before the model screening. These mixtures were encapsulated into w/o/w double emulsion droplets, reacted

with substrate 2 (0.5 mM) at 37 °C for 30 min and loaded on a flow cytometer (Supporting Information S8). Droplets with higher blue fluorescence were sorted into 2 mL Eppendorf tubes containing 0.2 mL LB medium and positive cells were recovered by plating on agar. GkaP-26A8-expressing cells and inactive cells were identified by testing the activity of recovered clones in 96-well plates. The enrichment factors were calculated by dividing the positive ratios after sorting by the positive ratios before sorting.

Evaluation of FDE Behavior of Substrates 14 and 15 in Droplets. In order to test the FDE behavior of substrates 14 and 15, *E. coli* BL21 (DE3) Codon Plus strain (Stratagene) expressing an esterase AFEST (in pET28a-AFEST plasmid)¹¹ and *E. coli* 10G strain (Lucigen) expressing the β -galactosidase Abg (in pKTnd-Abg plasmid)²³ were used as model enzymes. After encapsulation of single cells in w/o/w double emulsion droplets, cells were lysed by mixing the double emulsions with an equal volume of BugBuster and incubated for 10 min at 37

°C. Next, 10 μL substrate solutions of **14** or **15** (10 mM in DMSO) were added to 200 μL of the lysed cell mixture and incubated at 37 °C. For flow cytometry detection, the fluorescence of the reaction product, **16**, was detected in the Alexa Fluor 430 channel, with an excitation laser at 375 nm and a band-pass filter of 530/30 nm.

RESULTS AND DISCUSSION

Determination of the Critical Hydrophobicity for Oil Permeability. The permeability of a small molecule through the oil phase of a w/o/w microdroplet would be expected to depend upon its hydrophobicity. In order to explore this behavior in the context of coumarin fluorophores, we evaluated a small series of coumarin analogues. Cyano, carboxylic, and methyl sulfonate groups were introduced onto the 3- or 4-position of 7-hydroxycoumarin to generate three coumarins (**4**, **6**, **13**) with different hydrophobicities (Figure 1). The molecular hydrophobicity of each compound can be quantified by the partition coefficient ($\log D$), which is a measure of the differential solubility of a compound between water and octanol.²¹ The compounds were encapsulated into w/o/w double emulsions and their diffusion out of the droplets was monitored by flow cytometry. The w/o/w double emulsions were prepared by employing our previously developed membrane-extrusion method.¹¹ The membrane-extrusion protocol can generate droplets with significantly improved uniformity than those made by homogenizing method.³ Also, the membrane-extrusion protocol is more convenient and easier to operate than the emerging microfluidic method where complicated device setup is required,^{24–26} although the latter could provide even better droplet uniformity.

To mimic the sorting conditions in an IVC-FACS screening experiment, w/o/w double emulsion droplets containing 100 μM fluorophores in the inner water phase were diluted 100-fold and incubated at room temperature. As shown in Figure 2, the fast leakage of **4** caused serious cross-talk between droplets, which is indicated by a broad peak in the histogram (Figure 2A). As the broadening is a result of the diffusion/exchange, a measure of the width of this peak can be used to indicate the degree of the cross-talk. The width was measured by the proportion of the population showing a fluorescence signal of <0.33 or >3.0 times the mean fluorescence, which is 34% in Figure 2A. Of equal concern is the fact that the relative fluorescence intensity decreased more than 50% within 1 min (Figure 2D), indicating fast leakage of the fluorophore out of the droplets. This made **4** unsuitable for screening. The addition of a carboxylic acid group (as in **6**), however, resulted in much better retention in the droplets. Only 3.9% of the population showed a fluorescence outside the 3-fold limits (Figure 2B), and more than 70% of the fluorescence intensity remained after incubation for 1 h (Figure 2E). Compound **13**, containing a sulfate group, showed even better droplet retention, with only 1.2% of the droplets outside the limits (Figure 2C) and more than 90% of the fluorescence intensity retained after 1 h of incubation (Figure 2F). The order of retention of the three coumarins, $4 < 6 < 13$, is in accordance with their decreasing hydrophobicities. Fluorescent signal stabilities for both **6** ($\log D -5.92$) and **13** ($\log D -2.41$) are sufficient for 1 h of continuous IVC-FACS screening, and thus, for practical purposes, they can be considered as oil impermeable while **4** ($\log D 1.67$) is highly oil permeable. From this we conclude, as a first guide, that compounds with $\log D$

value >1.67 will pass through the oil phase while those with $\log D$ value < -2.41 will not.

Ostafe and co-workers have used a hydrophobic octanol group to deliver the polar glucose into the inner water phase,⁷ but it remains unclear how large a hydrophobic group is needed for efficient delivery. To solve this problem, the above-mentioned coumarins were converted into phosphotriesterase (PTE) substrates for the test. We calculated the $\log D$ values for such substrates in which a diethoxyphosphoryl group has been added to each fluorophore (Figure 1). The predicted hydrophobicities of substrates **1** ($\log D 2.66$), **2** ($\log D -2.13$), and **3** ($\log D -4.59$) were somewhat increased compared with the parent fluorophores, but it was not clear whether these changes would be sufficient (Figure 1). The oil permeability of each substrate was thus tested by adding them to the outer water phase of w/o/w double emulsion droplets that contained PTE in the inner water phase. If the compound passes through the oil phase and reacts with the enzyme, a fluorescence enhancement will be observed. This was tested using a highly active GkaP-26A8 mutant.²² After 60 min of incubation, both substrates **1** and **2** showed obviously increased fluorescence signals, suggesting their successful delivery into the droplets. However, there was almost no reaction with substrate **3** under these conditions (Supporting Information S7), indicating that the high hydrophilicity of this substrate prevented it from passing through the oil phase into the inner water phase. Given the $\log D$ values of these compounds (Figure 1), it seems that a substrate with $\log D$ value > -2.13 can pass through the oil phase from the outer water phase. Combining these results with our previous finding, the “critical $\log D$ value” for oil permeability can be narrowed down from -2.13 to -2.41 ; that is, if the $\log D$ value of a compound is greater than -2.13 , in practice it can pass through the oil phase, and if its $\log D$ value is smaller than -2.41 , it will not significantly pass through the oil phase. This “critical $\log D$ value” is an important parameter to control the “retention” and “pass through” behavior of compounds in w/o/w double emulsion droplets, but it is system-dependent and will likely be different if another oil phase is used. However, this parameter can be easily determined using equivalent methods.

Compound 2 Is an Effective FDE Substrate for IVC-FACS of Phosphotriesterase. These three substrates were then evaluated using w/o/w double emulsion droplets encapsulating GkaP-26A8-expressing *E. coli* single cells. In light of the previous results, substrates **1** and **2** were added to the outer water phase, while impermeable substrate **3** was mixed with the cell suspension before encapsulation. As seen in Figure 3, the high hydrophobicity of **4** resulted in rapid leakage of fluorescence throughout the droplets resulting in a merging of the populations of active and empty droplets that renders substrate **1** unsuitable for IVC-FACS assays. By contrast, the requirement for premixing of the highly hydrophilic, oil-impermeable substrate **3** resulted in a high fluorescence background due to reaction that occurred prior to encapsulation. Substrate **2**, on the other hand, seems to be sufficiently hydrophobic to pass through the oil phase, allowing it to be added to the outer water phase, thereby avoiding the fluorescence background associated with premixing prior to encapsulation. More importantly, the reaction product of substrate **2** (compound **6**) with its relatively higher hydrophilicity, is retained inside the w/o/w double emulsion droplets, decreasing both cross-talk between droplets and loss from them, thereby increasing the accuracy of IVC-FACS

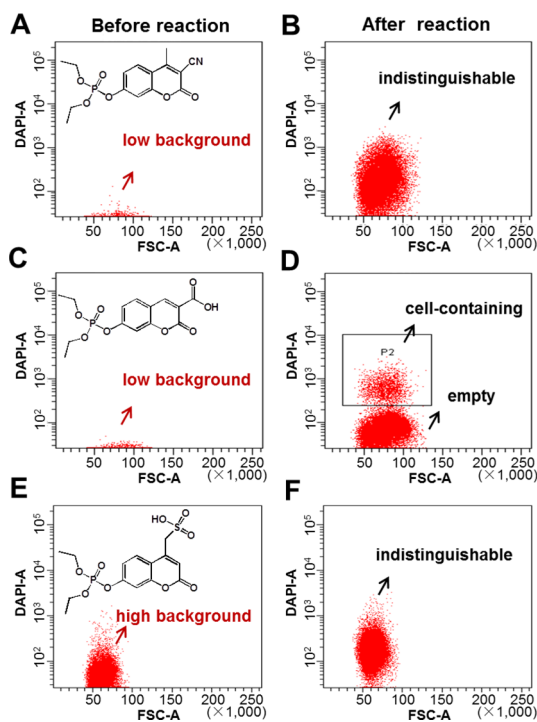


Figure 3. Hydrolysis of substrates 1, 2, and 3 by GkaP-26A8-expressing *E. coli* cells in w/o/w double emulsion droplets. Before reaction, substrates 1 and 2 showed very low fluorescence background (A, C) while background for substrate 3 was much higher (E). After incubation for 60 min, fluorescence increased for all three reactions (B,D,F). However, the discrimination between cell-containing droplets and empty ones was poor for 1 (B) due to rapid product leakage from the droplets. For 3, the boundary between cell-containing droplets and empty ones was also obscure due to the high fluorescence background before reaction (F). Only for 2 can the fluorescence of cell-containing droplets be clearly distinguished from that deriving from empty ones. Intact cells were encapsulated at a concentration of ~ 0.1 cell per droplet. Note: substrates 1 and 2 were added to the outer water phase, while oil impermeable substrate 3 was mixed with the cell suspension before single cell encapsulation. For each sample, approximately 20 000 droplets were analyzed.

assays. It should be noted that the FDE effect enabled by substrate 2 is not only about the delivery of substrate through the oil phase, which has been reported by our and other's previous work,^{3,7,11} it is equally important to control the property of the product to ensure the droplet retention of fluorescent signal. An overview of the performance of the three substrates and their corresponding products is provided in Figure 4.

Since many directed evolution studies have been performed on phosphotriesterases (PTEs), the development of efficient screening methods for this class of enzymes has attracted considerable attention.^{10,22} Gupta et al. applied IVC-FACS to evolution of the activity of mammalian serum paraoxonase PON1 toward S_p -cyclosarin, but the substrate they used (DEPCyC) was not ideal because the reaction product exchanged very quickly between droplets.¹⁰ We thus carried out studies to determine whether substrate 2 performed better in IVC-FACS screening, using a phosphotriesterase from *Geobacillus kaustophilus* HTA426 (GkaP) and three of its higher activity mutants 26A8, 26A8Y, and 26A8C. First, the relative activities of GkaPs toward substrate 2 and the commonly used PTE substrate paraoxon were measured in

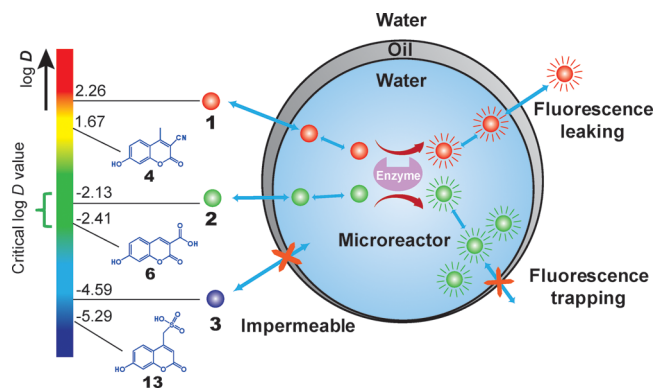


Figure 4. Scheme illustrating the different behavior of substrates 1, 2, and 3 in the w/o/w double emulsion droplets. The permeability of coumarin derivatives into and out of w/o/w double emulsion droplets is related to their hydrophobicity: the higher the $\log D$ value, the more easily they pass through the oil phase. Substrates 1 and 2 both diffuse into the inner water phase and undergo enzymatic cleavage, while 3 is too hydrophilic to enter and has to be premixed with the cell suspension prior to droplet generation. Coumarin 4, the product of cleavage of 1, is hydrophobic enough to rapidly diffuse out of the droplets, resulting in *fluorescence leaking*. In contrast 2, the product of compound 6 cleavage, is more hydrophilic and is retained. This behavior of substrate 2 in droplets is termed *fluorescence droplet entrapment (FDE)*.

1 \times PBS (pH 7.4) at 37 °C. As shown in Figure 5A, the relative activities measured with substrate 2 and paraoxon were very

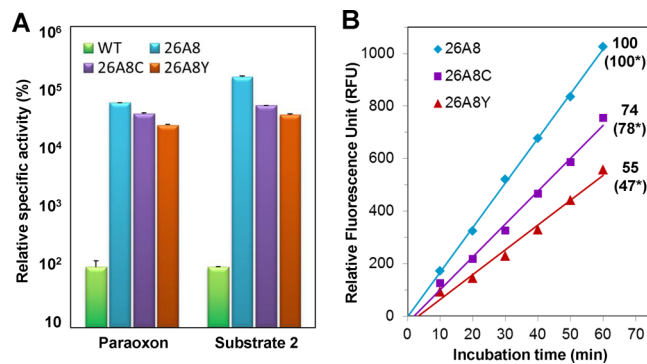


Figure 5. Characterization of 2 as a phosphotriesterase substrate. (A) Relative activities of GkaP wild-type enzyme and three mutants (26A8, 26A8Y, and 26A8C) toward paraoxon and substrate 2. For each substrate, the specific activities of the mutants were normalized to that of wild-type GkaP. (B) The IVC-FACS assay of *E. coli* cells expressing GkaP mutants (26A8, 26A8C and 26A8Y) using substrate 2. Intact cells were encapsulated at a concentration of ~ 0.1 cell per droplet and the fluorescence intensities versus reaction time were measured by flow cytometry. Their relative activities in this assay are shown and compared with those measured in free solution (number with asterisk). All the reactions were carried out in 1 \times PBS (pH 7.4) at 37 °C.

similar, indicating that substrate 2 could substitute for paraoxon as a screening substrate. In order to confirm that these results translated into the FACS assay, GkaPs-expressing *E. coli* cells were encapsulated in droplets, reacted with substrate 2, and assayed by flow cytometry. As can be seen in Figure 5B, linear time courses were obtained, indicating a good dynamic range for this assay. Further, the relative activities measured from the

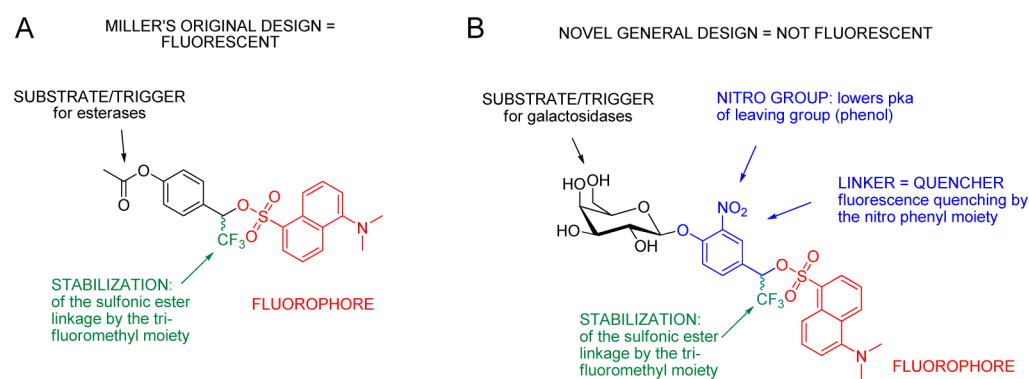


Figure 6. Design of Miller's fluorescent probe for esterases (A) and our novel design for the FDE substrate for galactosidases (B).

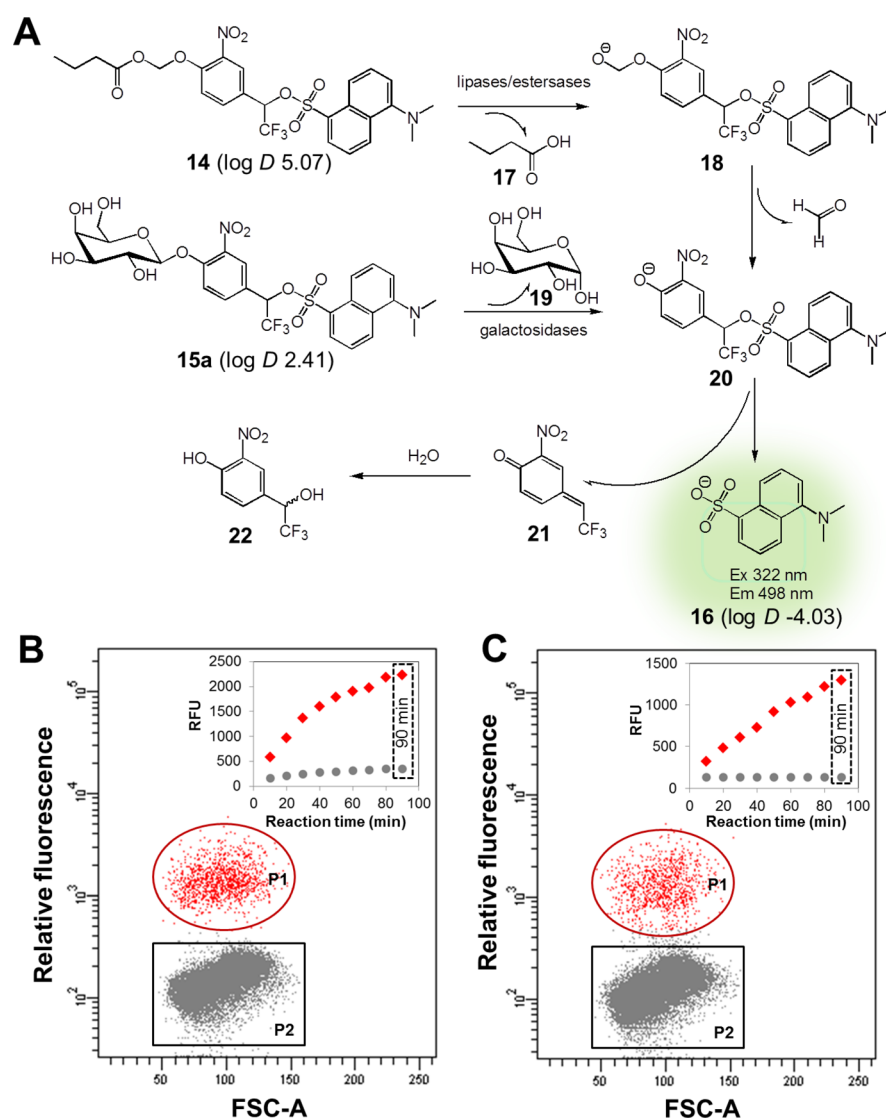


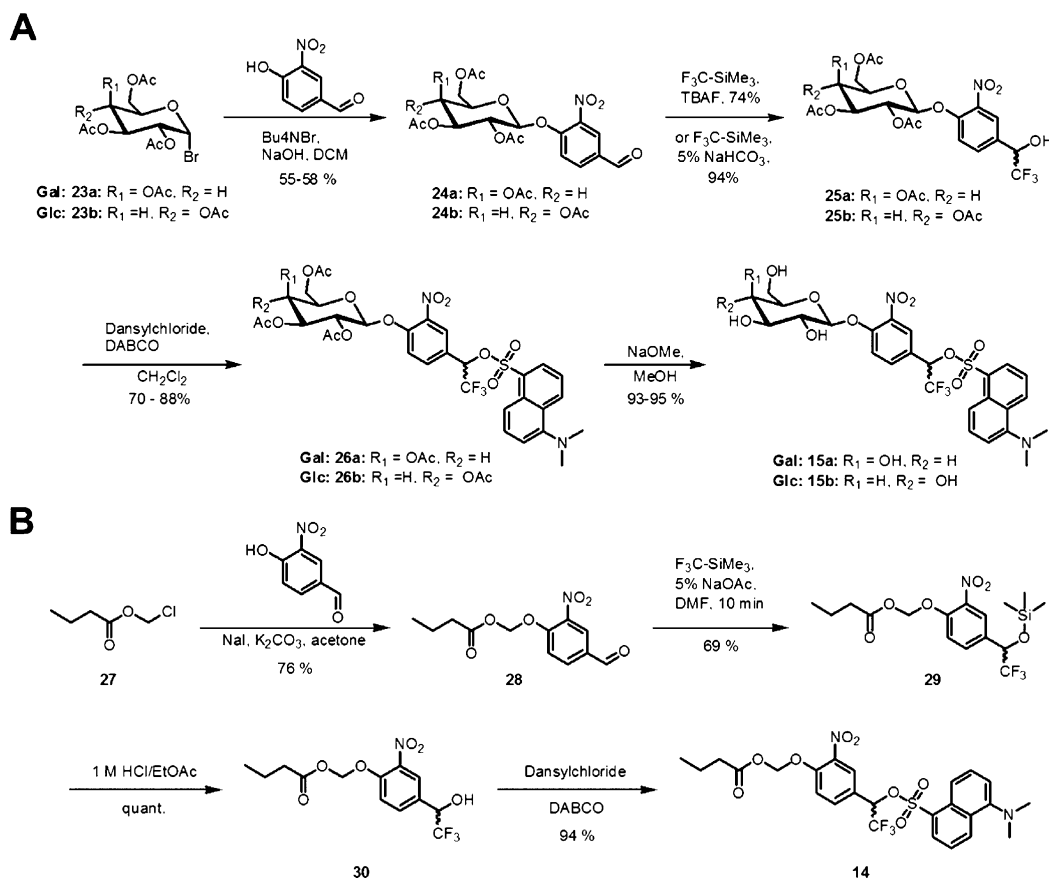
Figure 7. (A) Use of profluorogenic substrates for the assay of esterases and galactosidases. After hydrolysis, the intermediate released undergoes a decomposition step releasing the sulfonated fluorophore **16**. (B) Flow cytometry assay of esterase-expressing cells using substrate **14** in droplets. (C) Flow cytometry assay of galactosidase-expressing cells using substrate **15a** in droplets. In (B) and (C), the dot-plots show the fluorescence intensity of both cell-containing droplets (P1, red dots) and empty droplets (P2, gray dots) at a reaction time point of 90 min. Time courses for the reactions are shown in insets in the top right corners.

slope were consistent with those measured in bulk reactions, indicating that droplet assays based on substrate **2** are reliable.

To further evaluate the screening capability of the IVC-FACS system based on substrate **2**, a model screening of PTE-active

cells was carried out. *E. coli* cells expressing GkaP-26A8 were spiked into a large excess of PTE-inactive cells at different ratios before being encapsulated into w/o/w double emulsion droplets. To increase the accuracy of screening, a red

Scheme 1. Chemical Synthesis of 15a and 15b (A), and 14 (B)



fluorescent protein, mCherry, was used as a fluorescent tag for cell-containing droplets (Supporting Information S6). After reaction with substrate 2 at 37 °C for 30 min, positive droplets were sorted (Supporting Information S8) and recovered on an agar plate. The enrichment factors were calculated as listed in Table S1. Initial mixtures containing 10% or 1% positive cells could be enriched to more than 97% purity after only one round of sorting. Even the sample containing only 0.1% of positive cells in the starting population was enriched to 90% purity (over 900-fold enrichment). These enrichment efficiencies surpass those in all previously published work on this system, where enrichment factors were usually in the range of 40- to 330-fold,^{3,4,7,11} thereby confirming the utility of substrate 2 for IVC-FACS ultrahigh throughput screening of PTEs.

Design of a General Fluorophore for FDE Substrates.

As shown above, the key of FDE strategy is to increase the hydrophobicity of the initial substrate to facilitate its diffusion while increasing the hydrophilicity of the fluorescent reporter to maintain it within the droplet following enzymatic activity. However, our initial design of the FDE substrates for PTEs is quite limited, because it was necessary to attach a highly hydrophobic enzyme-cleavable portion to sufficiently increase the overall hydrophobicity of the substrate. This design will not work for the screening of enzymes such as glycosidases that cleave more polar substrates. To improve upon the FDE effect of the first engineering strategy for a more diverse set of substrates, a new design is required involving a net hydrophobic substrate that releases a charged fluorophore upon cleavage. Initial attempts to generate such substrates focused on directly attaching the functional group that would become charged

upon enzymatic cleavage, to the anomeric center of the sugar. However, these substrates all proved to be too labile to be of practical use. It was thus necessary to attach the fluorophore to the sugar via some form of self-immolative linker in order to “insulate” the reactive leaving group from the anomeric center.

The approach that was ultimately successful (Figure 6) was inspired by the work from S. Miller who developed cell permeable “pro-fluorophores” that were released inside cells after cleavage by cellular esterases.²⁷ After enzymatic cleavage of the glycoside or ester, the highly polar and fluorescent dansyl acid 16 is liberated by a 1,6-benzylic elimination of intermediate 20 (Figure 7A). Fluorescent dansyl acid 16 is charged at physiological pH ($\text{p}K_a = 0.22 \pm 0.4$), with a log D value of -4.03 (predicted by online ACD/I-Lab prediction engine) and should thus be retained within the w/o/w double emulsion droplets. A key modification to Miller’s original design was the installation of a nitro group on the self-immolative linker to dramatically lower the $\text{p}K_a$ of the leaving group and increase rates of cleavage by glycosidases. An important additional point is that the nitrophenol moiety quenches the fluorescence of the dansyl ester moiety by a photoinduced electron transfer (PeT) mechanism,²⁸ which dramatically lowers the background fluorescence of the intact substrate about 200-fold (data not shown). A similar PeT mechanism has been used to increase the sensitivity of fluorescence probes in living cells.²⁹ Therefore, pro-fluorescent probes 14, 15a, and 15b function as “turn-on” fluorescent probes. Consequently there is no requirement to “wash out” excess substrate prior to sorting.

In the case of esterase substrate 14, an additional oxy-methylene group was inserted into the linker (Figure 7A).³⁰

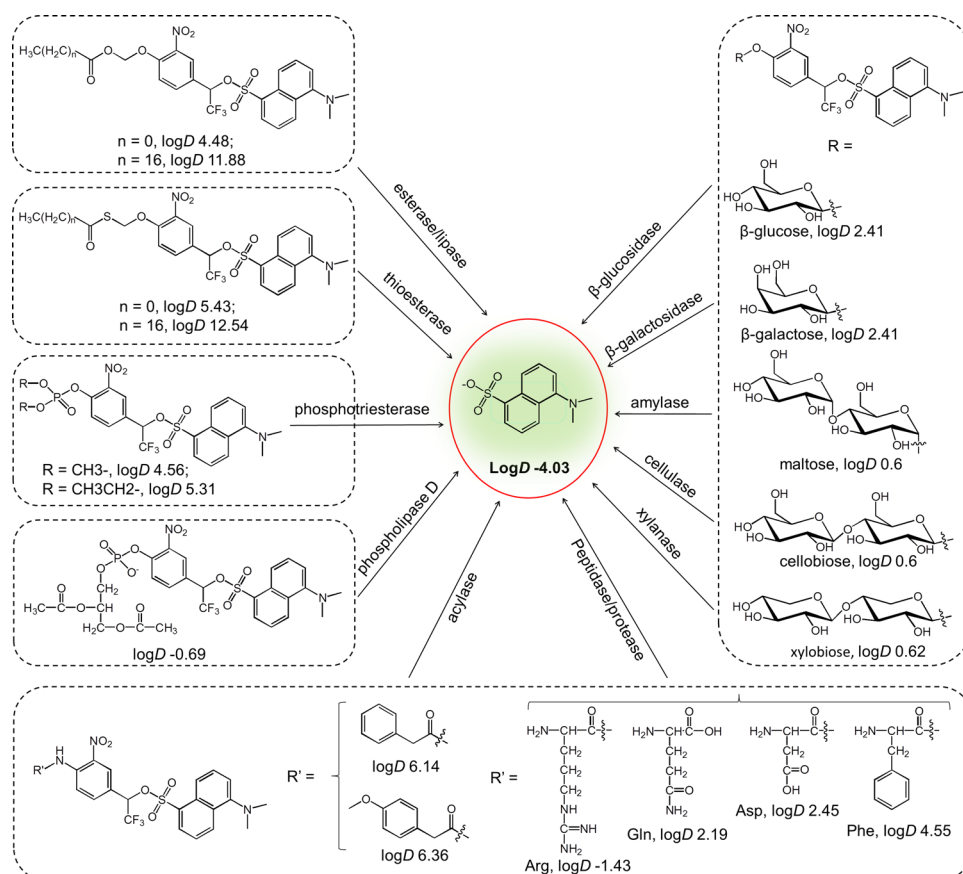


Figure 8. Proposed FDE substrates for various kinds of hydrolytic enzymes.

This modification converted an otherwise highly reactive and labile nitrophenolic ester bond into a stable phenolic ether. Hydrolysis of the enzymatic trigger group thus releases hemiacetal **18** which decomposes spontaneously (Figure 7A). Subsequently, the self-immolative linker liberates the dansyl acid **16**. The synthesis of profluorogenic probes **15a**, **15b**, and **14** is outlined in Scheme 1 and described in detail in the Supporting Information S2. In brief, glycosylation of the glycosyl bromides **23** under phase transfer catalysis yielded the formylaryl glycosides **24** (Scheme 1A).³¹ The trifluoromethylation of the aldehyde functionality with the Ruppert–Prakash reagent³² gave the corresponding glycosides **25** in high yield. Conversion of alcohols **25** into dansyl ester **26** with dansyl chloride followed by Zemplén saponification yielded the profluorescent probes **15** in excellent yield. Notably, the stabilizing influence of the trifluoromethyl group allowed a basic deprotection of the acetyl groups in the presence of one of the more reactive leaving groups in organic chemistry.^{33,34}

For the synthesis of profluorogenic probe **14**, chloromethyl butyrate **27** was reacted with 4-hydroxy-3-nitrobenzaldehyde to yield arylmethyl butyrate **28**. Subsequently, the aldehyde functionality of **28** was trifluoromethylated to yield silylated alcohol **29**.³² The trimethylsilyl group was extraordinarily stable and was cleaved off by prolonged stirring of **29** in a biphasic 1 M HCl/ethyl acetate solution, demonstrating the stabilizing influence of the trifluoromethyl group again.^{33,34} Reacting alcohol **30** with dansyl chloride gave the profluorogenic probe **14** in 49% overall yield (4 steps).

The performance of the newly designed fluorophore and its corresponding galactosidase and esterase substrates were tested

in the w/o/w double emulsion droplets. As was hoped, charged fluorophore **16** showed exceptional fluorescent stability in the droplet (see Supporting Information S9 for detail). Also as hoped, masking of the sulfonate by the enzyme-labile groups resulted in greatly increased hydrophobicity that allows transport of both substrates into the inner water phase. When the substrates were loaded in the outer water phase of the w/o/w droplets containing *E. coli* cells expressing an esterase or a galactosidase, a strong fluorescence signal developed in the inner layer of the droplets for both substrates (Figure 7B,C). The enzymatic reaction in the droplets is easily distinguished from the empty droplets with good dynamic range, indicating a clear FDE effect that ensures a reliable IVC-FACS assay.

This substrate engineering strategy for the design of IVC-FACS substrates should be reasonably broadly applicable to a range of hydrolytic enzymes. In that light, we propose substrates of appropriate predicted polarities for a range of important enzymes, including phospholipases, acylases, peptidases, proteases, xylanases and cellulases (Figure 8). The availability of more FDE substrates will propel the development of high efficiency IVC-FACS assays that in turn will generate enzymes of greater utility.

CONCLUSIONS

In conclusion, we have proposed a new substrate design strategy for IVC-FACS screening of enzymatic activities. The so-called fluorescence droplet entrapment (FDE) approach is based on an oil-diffusible, fluorogenic substrate that, upon enzymatic cleavage, liberates a less diffusible, fluorescent

product, which is retained within a single droplet. FDE provides accurate control of the reaction timing, minimizes cross-talk between mutants, and yields a low fluorescence background. Although described here only for the IVC-FACS screening of three hydrolytic enzymes, the FDE strategy can be extended to the engineering of other enzymes and antibodies^{32,33} that benefit from the characterization of single clones, thereby facilitating biotechnological approaches for the production of biofuels, chemicals and pharmaceuticals.

■ ASSOCIATED CONTENT

● Supporting Information

The Supporting Information is available free of charge on the ACS Publications website at DOI: [10.1021/acs.analchem.6b01712](https://doi.org/10.1021/acs.analchem.6b01712).

Additional information as noted in text (PDF)

■ AUTHOR INFORMATION

Corresponding Author

*E-mail: yanggy@sjtu.edu.cn. Tel: (+86)21-34205079. Fax: (+86)21-34207189.

Present Address

§(M.F.) Sandoz GmbH, Biochemiestrasse 10, A-6250 Kundl, Tyrol, Austria

Notes

The authors declare no competing financial interest.

■ ACKNOWLEDGMENTS

This work is supported by National Basic Research Program of China (973 Program, grant no. 2012CB721000), National Natural Science Foundation of China (grant nos. 31470788 and 31100611), the Natural Sciences and Engineering Research Council of Canada, Genome Canada, and Genome British Columbia. F.M. was supported by the Ph.D. Scholarship for Visiting Aboard granted by Shanghai Jiao Tong University. M.F. thanks the Austrian Science Fund (FWF) for an Erwin Schrödinger Fellowship (J3293-B21). The authors thank Qian Luo and Xinde Zhu in Instrument & Service Center of School of Life Sciences and Biotechnology, Shanghai Jiao Tong University for flow cytometry service.

■ REFERENCES

- (1) Turner, N. J. *Nat. Chem. Biol.* **2009**, *5*, 567–573.
- (2) Bornscheuer, U.; Huisman, G.; Kazlauskas, R.; Lutz, S.; Moore, J.; Robins, K. *Nature* **2012**, *485*, 185–194.
- (3) Aharoni, A.; Amitai, G.; Bernath, K.; Magdassi, S.; Tawfik, D. S. *Chem. Biol.* **2005**, *12*, 1281–1289.
- (4) Mastrobattista, E.; Taly, V.; Chanudet, E.; Treacy, P.; Kelly, B. T.; Griffiths, A. D. *Chem. Biol.* **2005**, *12*, 1291–1300.
- (5) Ostafe, R.; Prodanovic, R.; Commandeur, U.; Fischer, R. *Anal. Biochem.* **2013**, *435*, 93–98.
- (6) Hardiman, E.; Gibbs, M.; Reeves, R.; Bergquist, P. *Appl. Biochem. Biotechnol.* **2010**, *161*, 301–312.
- (7) Ostafe, R.; Prodanovic, R.; Nazor, J.; Fischer, R. *Chem. Biol.* **2014**, *21*, 414–421.
- (8) Hwang, B.-Y. *Biotechnol. Bioprocess Eng.* **2012**, *17*, 500–505.
- (9) Tu, R.; Martinez, R.; Prodanovic, R.; Klein, M.; Schwaneberg, U. *J. Biomol. Screening* **2011**, *16*, 285–294.
- (10) Gupta, R. D.; Goldsmith, M.; Ashani, Y.; Simo, Y.; Mullokandov, G.; Bar, H.; Ben-David, M.; Leader, H.; Margalit, R.; Silman, I.; Sussman, J. L.; Tawfik, D. S. *Nat. Chem. Biol.* **2011**, *7*, 120–125.

- (11) Ma, F.; Xie, Y.; Huang, C.; Feng, Y.; Yang, G. *PLoS One* **2014**, *9*, e89785.
- (12) Bjerregaard, S.; Pedersen, H.; Vedstesen, H.; Vermehren, C.; Söderberg, I.; Frokjaer, S. *Int. J. Pharm.* **2001**, *215*, 13–27.
- (13) Pays, K.; Giermanska-Kahn, J.; Pouligny, B.; Bibette, J.; Leal-Calderon, F. *J. Controlled Release* **2002**, *79*, 193–205.
- (14) Cheng, J.; Chen, J.-F.; Zhao, M.; Luo, Q.; Wen, L.-X.; Papadopoulos, K. D. *J. Colloid Interface Sci.* **2007**, *305*, 175–182.
- (15) Wen, L.; Papadopoulos, K. D. *Colloids Surf., A* **2000**, *174*, 159–167.
- (16) Courtois, F.; Olguin, L. F.; Whyte, G.; Theberge, A. B.; Huck, W. T.; Hollfelder, F.; Abell, C. *Anal. Chem.* **2009**, *81*, 3008–3016.
- (17) Huque, F. T.; Jones, K.; Saunders, R. A.; Platts, J. A. *J. Fluorimetry Chem.* **2002**, *115*, 119–128.
- (18) Studer, A.; Hadida, S.; Ferritto, R.; Kim, S.-Y.; Jeger, P.; Wipf, P.; Curran, D. P. *Science* **1997**, *275*, 823–826.
- (19) Wu, N.; Courtois, F.; Zhu, Y.; Oakeshott, J.; Easton, C.; Abell, C. *Electrophoresis* **2010**, *31*, 3121–3128.
- (20) Najah, M.; Mayot, E.; Mahendra-Wijaya, I. P.; Griffiths, A. D.; Ladame, S.; Drevelle, A. *Anal. Chem.* **2013**, *85*, 9807–9814.
- (21) Woronoff, G.; El Harrak, A.; Mayot, E.; Schicke, O.; Miller, O. J.; Soumillion, P.; Griffiths, A. D.; Ryckelynck, M. *Anal. Chem.* **2011**, *83*, 2852–2857.
- (22) Zhang, Y.; An, J.; Ye, W.; Yang, G.; Qian, Z.-G.; Chen, H.-F.; Cui, L.; Feng, Y. *Appl. Environ. Microbiol.* **2012**, *78*, 6647–6655.
- (23) Kim, Y.-W.; Lee, S. S.; Warren, R. A. J.; Withers, S. G. *J. Biol. Chem.* **2004**, *279*, 42787–42793.
- (24) Zinchenko, A.; Devenish, S. R.; Kintsjes, B.; Colin, P. Y.; Fischlechner, M.; Hollfelder, F. *Anal. Chem.* **2014**, *86*, 2526–2533.
- (25) Yan, J.; Bauer, W.-A.; Fischlechner, C. M.; Hollfelder, F.; Kaminski, C. F.; Huck, W. T. *Micromachines* **2013**, *4*, 402–413.
- (26) Lim, S. W.; Abate, A. R. *Lab Chip* **2013**, *13*, 4563–4572.
- (27) Rusha, L.; Miller, S. C. *Chem. Commun.* **2011**, *47*, 2038–2040.
- (28) Lakowicz, J. R. *Principles of Fluorescence Spectroscopy*, 3rd ed.; Springer: New York, 2006; p 954.
- (29) Izumi, S.; Urano, Y.; Hanaoka, K.; Terai, T.; Nagano, T. *J. Am. Chem. Soc.* **2009**, *131*, 10189–10200.
- (30) Lavis, L. D.; Chao, T.-Y.; Raines, R. T. *Chem. Sci.* **2011**, *2*, 521–530.
- (31) Kröger, L.; Thiem, J. *Carbohydr. Res.* **2007**, *342*, 467–487.
- (32) Prakash, G. S.; Yudin, A. K. *Chem. Rev.* **1997**, *97*, 757–786.
- (33) Allen, A. D.; Ambidge, I. C.; Che, C.; Micheal, H.; Muir, R. J.; Tidwell, T. *J. Am. Chem. Soc.* **1983**, *105*, 2343–2350.
- (34) Miller, S. C. *J. Org. Chem.* **2010**, *75*, 4632–4635.